Journal of Sol-Gel Science and Technology 23, 231–234, 2002

Optical Properties of $Mg_xZn_{1-x}O$ Polycrystalline Thin Films Prepared by Sol-Gel Deposition Method

DONGXU ZHAO, YICHUN LIU*, DEZHEN SHEN, YOUMING LU, JIYING ZHANG AND X.W. FAN
Laboratory of Excited State Processes, Chinese Academy of Sciences, Changchun Institute of Optics, Fine Mechanics and Physics, Chinese Academy of Sciences, 1-Yan An Road, Changchun, 130021, P.R. China
liuyichun@mail.china.com

Received March 21, 2001; Accepted August 13, 2001

Abstract. The $Mg_xZn_{1-x}O$ alloy thin films were synthesized on Si and quartz substrates by the sol-gel deposition method. The transmittance and cathodoluminescence spectra of the $Mg_{0.05}Zn_{0.95}O$ and $Mg_{0.15}Zn_{0.85}O$ nanoparticle films were obtained at room temperature. It was found that the bandgap of $Mg_{0.05}Zn_{0.95}O$ and $Mg_{0.15}Zn_{0.85}O$ films is as large as 3.72 eV and 3.79 eV, respectively. The ultraviolet emission peaks are located at 376 nm and 370 nm, respectively, for the samples annealed at 600°C. When the annealing temperature is elevated to 1000°C, the band-gap decreases to 3.42 eV and an emission line related to the deep-level defect appears at 500 nm. The mechanism behind these phenomena is discussed.

Keywords: sol-gel method, $Mg_xZn_{1-x}O$ alloy, thin film, optical properties

1. Introduction

ZnO is a wide band-gap semiconductor ($E_g \approx 3.2$ eV) with a high exciton binding energy of 60 meV at room temperature. ZnO films have been extensively studied for use in transparent conducting electrodes in solar cells, flat panel displays, surface acoustic wave devices, and chemical sensors. Since Tang *et al.* obtained the ultraviolet lasing from ZnO thin films in 1997, ZnO films have attracted considerable attention as a possible candidate among wide-gap semiconductors for short-wavelength light-emitting devices (LEDS). Furthermore, ZnO films have been considered as a substrate for GaN [1–3]. Both these materials have the same crystal structure (wurtzite), but ZnO is more superior to GaN in some physical features. For example, ZnO is a relatively hard and stable material because the strength of the Zn—O—Zn bond is larger than that of the Ga—N—Ga bond and ZnO has a melting point of about 2000°C [4].

To obtain more efficient and potentially useful ultraviolet emitting devices based on ZnO, it is very important to construct a heterojunction which can realize double confinement actions for electrons and photons in optoelectronic devices. Thus, it is necessary to find a material with a wider band-gap and crystal structure comparable to ZnO. Doping with other ions is a popular and efficient way in ZnSe and GaN based devices [5, 6]. ZnO films doped with Mg^{2+} ions are often studied, because the ionic radius of Mg^{2+} (0.57 Å) is similar to that of Zn^{2+} (0.60 Å) and the band gap of MgO is about 7.7 eV [7]. Heterojunctions based on these materials were fabricated successfully using different methods [8, 9]. The $Mg_xZn_{1-x}O$ films have the basic structure of ZnO with x up to 0.46 and the band gap ranges from 3.24 to 4.2 eV [10].

The sol-gel deposition technique is a more convenient and cheaper way to fabricate thin films. The components of the film are changed easily by adjusting the different ion proportions in the sol. We have obtained $Mg_xZn_{1-x}O$ thin films by this method. The alloy thin films keep the ZnO wurtzite structure with the

*To whom all correspondence should be addressed.

x value up to 0.36 after annealing at 700°C. The band gap ranges from 3.4 to 3.93 eV ($0 \leq x \leq 0.36$) [11].

In this paper, two series of $Mg_xZn_{1-x}O$ films grown on Si (100) and quartz substrates by the sol-gel deposition method are examined. The transmittance and cathodoluminescence spectra were employed to probe the optical properties of the $Mg_{0.05}Zn_{0.95}O$ and $Mg_{0.15}Zn_{0.85}O$ nanoparticle films after thermal treatment at different temperatures.

2. Film Preparation

The alloy thin films were synthesized on Si (001) and quartz substrates by the sol-gel deposition method. The sol was composed of $Zn(CH_3COO)_2$, $Mg(CH_3COO)_2$ and polyvinyl butyral (PVB) in an ethanol solution. The total concentration of metal ions was fixed at 0.1 mol/L. The concentration of Mg^{2+} was adjusted to 0.01 and 0.02 mol/L. The solution was spin-coated on Si (100) and quartz substrates at 2500 rpm. After the deposition, the substrates were first heated to 100°C in air for 10 minutes in order to evaporate the solvent, then at 350°C in O_2 for half an hour in order to eliminate the organic component in the film. This process was repeated many times until the desired thickness was reached. The sample was then cut into several pieces for use in different experiments. Finally, thermal annealing was performed for one hour in an O_2 environment at different temperatures ranging from 500°C to 900°C in order to crystallize the zinc oxide film. The infrared spectrum was measured by a BIO-RAD FTS-3000 spectrophotometer with a resolution of 4 cm^{-1} in the range 400–4000 cm^{-1}, which indicated that there was not any organic component in the film above 350°C.

The XRD was measured by a D/max-rA x-ray diffractometer (Rigaku) using Cu K_α of 1.5418 Å to determine the crystal structure. A UV-360 Spectrophotometer (Shimadzu) was used for the optical characterization. The x value in the $Mg_xZn_{1-x}O$ films was found to be 0.05 and 0.15 from the analysis of the energy spectrum.

3. Results and Discussion

Figure 1 shows the XRD spectra of the $Mg_{0.05}Zn_{0.95}O$ and $Mg_{0.15}Zn_{0.85}O$ thin films with annealing temperatures of 350°C, 500°C, 600°C, 700°C, 800°C, 900°C and 1000°C. From Fig. 1, it can be seen that the films seem almost amorphous when the annealing temperature is below 500°C. When the annealing temperature is as high as 600°C, three peaks appear corresponding to the (100), (002) and (101) planes of ZnO with a wurtzite structure. All the films are well oriented to the c-axis without any peaks related to MgO. As the annealing temperature is increased, the orientation along (002) of the hexagonal crystal structure becomes stronger and the full width at half maximum (FWHM) of the (002)-ZnO peak becomes narrower.

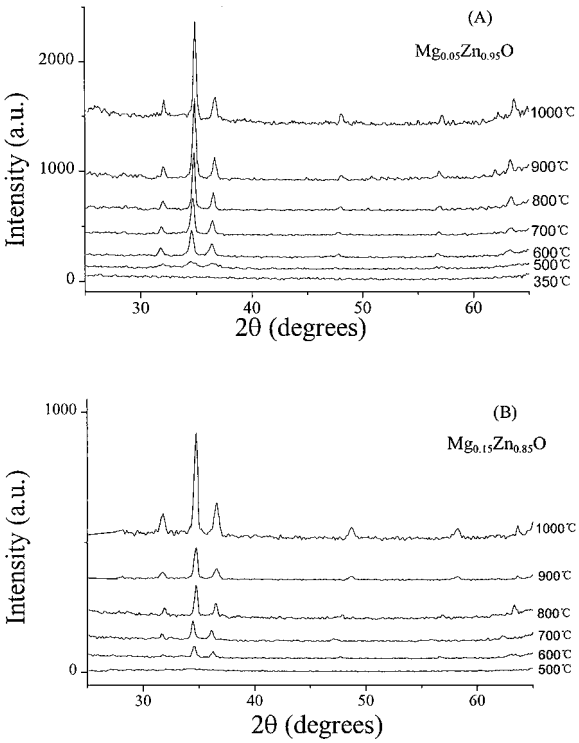

Figure 1. The X-ray diffraction patterns of $Mg_{0.05}Zn_{0.95}O$ and $Mg_{0.15}Zn_{0.85}O$ thin films on Si (001) substrate annealed at different temperatures.

The transmittance spectra of these two series of $Mg_xZn_{1-x}O$ thin films were measured in the ultraviolet-visible region at room temperature in order to determine the band gap (E_g) from the relationship $a^2 \propto (h\nu - E_g)$, where α is the absorption coefficient and $h\nu$ is the photon energy. This spectrum is shown in Fig. 2. The films were annealed at 350, 500, 600, 800, 900 and 1000°C on a quartz substrate for 1 hour in air. As discussed above, Fig. 2(A) suggests that the crystalline phase was formed after thermal treatment at 600°C. This is in agreement with the results obtained from X-ray diffraction (XRD) patterns. The films are transparent in the visible region of 400 to 800 nm and the absorbance edge of the films is

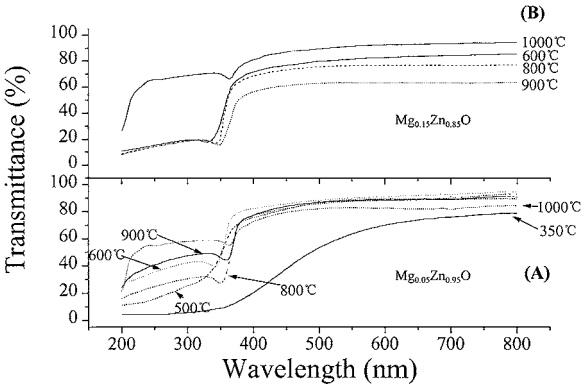

Figure 2. The trancemittance spectra of (A) $Mg_{0.05}Zn_{0.95}O$ and (B) $Mg_{0.15}Zn_{0.85}O$ thin films on quartz substrate annealed at different temperatures.

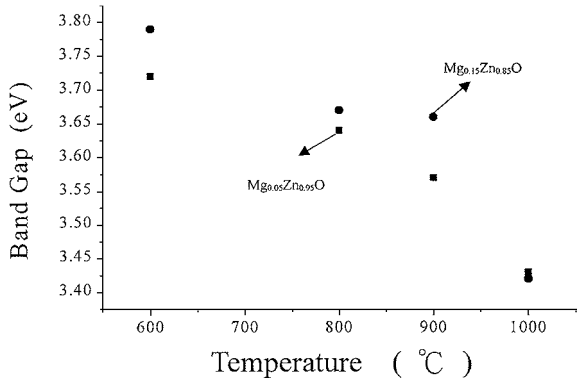

Figure 3. The band-gap of $Mg_{0.05}Zn_{0.95}O$ (●) and $Mg_{0.15}Zn_{0.85}O$ (■) films after annealing at temperature given on the horizontal axis.

red-shifted as the annealing temperature is increased. The film annealed at 1000°C is slightly different to the other films. Its transmittance is as high as 60% between 250 nm and 350 nm. The absorbance edge of the $Mg_{0.15}Zn_{0.85}O$ film is located at the higher energy side than the $Mg_{0.05}Zn_{0.95}O$ film under the same annealing temperature. The band gap (E_g) as a function of the annealing temperature is shown in Fig. 3. The E_g decreases as the annealing temperature is increased. At 1000°C the band gap of the $Mg_{0.05}Zn_{0.95}O$ and $Mg_{0.15}Zn_{0.85}O$ films is almost equal. This result is different to what has been previously reported [9]. The E_g value of $Mg_{0.15}Zn_{0.85}O$ films fabricated by laser molecular-beam epitaxy remained at a constant 3.56 eV for annealing temperatures ranging from 400°C to 1000°C. When the x value exceeded 0.15, the E_g of the alloy films decreased after annealing at a determined temperature.

The optical properties of the $Mg_xZn_{1-x}O$ thin film describe the nature of the band gap. The optical energy gap is correlated with the mean nanoparticle size and the number of various defects. In other words, there are two aspects which control the energy band: one is particle size (quantum-confinement effect), the other is the defect density. In order to evaluate the mean size of the $Mg_xZn_{1-x}O$ nanoparticles in the film, the Scherrer formula was employed to the $Mg_xZn_{1-x}O$ thin films:

$$t = \frac{0.9\lambda}{B\cos\theta_B}, \tag{1}$$

where λ, θ_B and B are the x-ray wavelength (1.54056 Å), Bragg diffraction angle, and full width at half maximum of the (002) peak around 34.64°, respectively [12]. The mean sizes of the $Mg_{0.05}Zn_{0.95}O$ nanoparticle are 5, 7, 10 and 12 nm for the samples annealed at 600, 700, 800, 900°C, respectively. This result indicates that the particle size increases with increasing annealing temperature. Due to the quantum-confinement effect, the band gap shifts to the low energy side with the increase of the particle size.

When increasing the thermal treatment temperature, some weak bonds are broken to form dangling bonds as the structural defects. These defects cause many local states to form local band tails in the conduction or valence band. As a result, the E_g deduced from the transmittance spectra decreases with the increase of annealing temperature. The results indicate that the E_g reduces rapidly after thermal-treatment at 1000°C. The defects present in the alloy thin films also affect the luminescence of the $Mg_xZn_{1-x}O$ alloy nanoparticle. The cathodoluminenscence spectra of the films measured at room temperature (10 KV, 7 μA) are shown in Fig. 4. The emission peaks are located at 387 nm, 376 nm and 370 nm for the un-doped ZnO, $Mg_{0.05}Zn_{0.95}O$ and $Mg_{0.15}Zn_{0.85}O$ samples, respectively, after being annealed at 600°C. No low energy transition is observed. These ultraviolet peaks exhibit a Stokes shift on the lower energy side of the adsorption edge. The broadening and Stokes shift of the luminescence peak are frequently observed in alloy semiconductors, where carriers experience different potentials depending on the local concentration and/or arrangement of the doping elements [7, 13]. This effect is larger in ZnO than in III-V semiconductors. When the annealing temperature is increased to 700°C, the three emission peaks are red-shifted to 394 nm, 383 nm and 381 nm, respectively.

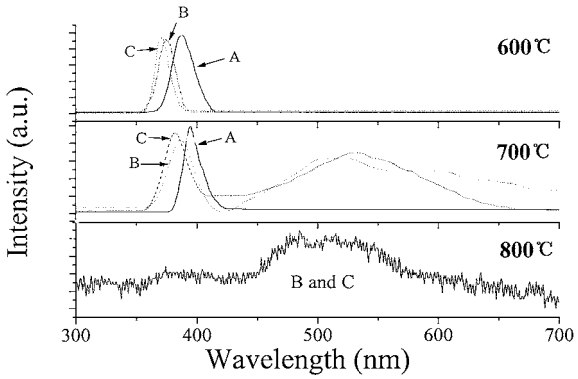

Figure 4. The cathodoluminescence spectra of (A) ZnO, (B) $Mg_{0.05}Zn_{0.95}O$ and (C) $Mg_{0.15}Zn_{0.85}O$ thin films on the Si (001) substrate heated at different temperatures.

At high annealing temperatures, another side-effect is the creation of deep defects induced by thermal fluctuation. It is also been proposed that annealing the samples in air at high temperature results in producing oxygen vacancies. In the $Mg_{0.05}Zn_{0.95}O$ and $Mg_{0.15}Zn_{0.85}O$ samples, a broad green emission line appears at 530 nm, which is attributed to the structural defect created by oxygen vacancies (Green Band) [14]. The intensity of the ultraviolet and blue region is almost the same. However, after the films are annealed above 800°C, there is only one broad peak at 500 nm in all of the samples and the emission peak in the ultraviolet region is much weaker than in the blue-green region. This indicates that the structural defect is dominant in the $Mg_xZn_{1-x}O$ alloy nanoparticle after a high temperature thermal treatment.

4. Conclusion

In conclusion, the ultraviolet emission from the $Mg_xZn_{1-x}O$ nanoparticle was obtained by cathode-ray excitation. It has been shown that the wavelength alters with the particle size at a low annealing temperature. A shorter emitted wavelength can be achieved by controlling the size and the component of the $Mg_xZn_{1-x}O$ nanoparticle. The green emission presents and dominates in the spectra when annealed at high temperature. This result shows that the structure defect density increases with enhancing the heated temperature of the sample. In order to obtain the strong UV emission of the $Mg_xZn_{1-x}O$ nanoparticle the proper annealing temperature is needed.

Acknowledgments

This work is supported by the Program of CAS Hundred Talents, The Innovation Project Item of Chinese Academy of Science, The Key Project of the National Natural Science Foundation of China No. 69896260 and the National Fundamental and Applied Research Project.

References

1. Z.K. Tang, P. Yu, G.K.L. Wong, M. Kawasaki, A. Ohtomo, H. Koinuma, and Y. Segawa, Solid State Commun. **103**, 459 (1997).
2. Z.K. Tang, G.K.L. Wong, P. Yu, M. Kawasaki, A. Ohtomo, H. Koinuma, and Y. Segawa, Appl. Phys. Lett. **72**, 3270 (1998).
3. Sunglae Cho, Jing Ma, Yunki Kim, Yi Sun, George K.L. Wong, and John B. Ketterson, Appl. Phys. Lett. **75**, 2761 (1999).
4. Y.R. Ryu, S. Zhu, J.D. Baudai, H.R. Chandrasekhar, P.F. Miceli, and H.W. White, J. Appl. Phys. **88**, 201 (2000).
5. H. Okuyama, K. Nakano, T. Miyajima, and K. Akimito, Jpn. J. Appl. Phys. **30**(2), L1620 (1991).
6. S. Nakamura and G. Fasol, *The Blue Laser Diode* (Springer, Berlin, 1997).
7. A. Ohtomo, M. Kawasaki, T. Koida, K. Masubuchi, H. Koinuma, Y. Sakural, Y. Yoshida, T. Yasuda, and Y. Segawa, Appl. Phys. Lett. **72**, 2466 (1998).
8. A.K. Sharma, J. Narayan, J.F. Muth, C.W. Teng, C. Jin, A. Kvit, R.M. Kolbas, and O.W. Holland, Appl. Phys. Lett. **75**, 3327 (1999).
9. A. Ohtomo, R. Shiroki, I. Ohkubo, H. Koinuma, and M. Kawasaki, Appl. Phys. Lett. **75**, 4088 (1999).
10. T. Minemoto, T. Negami, S. Nishiwaki, H. Takakura, and Y. Hamakawa, Thin Solid Film **372**, 173 (2000).
11. D.X. Zhao, Y.C. Liu, and D.Z. Shen, J. Crystal Growth, Submitted.
12. B.D. Cullity, *Elements of X-Ray Diffractions* (Addition-Wesley, Reading, MA, 1978), p. 102.
13. R. Zimmermann, J. Cryst. Growth **101**, 346 (1990).
14. K. Vanheusden, C.H. Seager, W.L. Warren, D.R. Tallant, and J.A. Voigt, Appl. Phys. Lett. **68**, 403 (1996).